Pis'ma v ZhETF, vol. 85, iss. 10, pp. 584 – 588 © 2007 May 25

On the role of dust in the cometary plasma

B. A. Klumov, S. V. Vladimirov, G. E. Morfill*

Max-Planck-Institut für Extraterrestrische Physik, D-85740 Garching, Germany

** School of Physics, The University of Sydney, New South Wales 2006, Australia*

Submitted 15 March 2007
Resubmitted 5 April 2007

The cometary coma consists of neutral gas, plasma, and dust grains. Dust grains can influence both the neutral and charged coma's constituents. Usually, presence of dust particles in a plasma results in additional losses of both electrons and ions due to the plasma recombination on the particle surfaces. Solar radiation makes the impact of dust even more complicated, depending on the solar flux, the dust number density, photoelectric properties of the dust particles, the dust particle composition, distribution of sizes, etc. We propose a simple kinetic model evaluating the role of dust particles in the coma plasma chemistry and demonstrate that this role can be crucial resulting in a nontrivial behavior of both the electron and ion densities of the plasma. We show that coma's dust particles can be negatively as well as positively charged depending on their composition. These opposite charges of the grains can result in fast coagulation of dust particles forming complex aggregate shapes of cometary grains.

PACS: 94.05.–a, 96.25.–y

The processes in a multi-component plasma containing dust particles attract considerable attention at present [1 – 3]. Interest in dusty plasma is stimulated by its great abundance in Nature, important role in laboratory and technological plasmas as well as by the significant (sometimes crucial) effect of dust particles on the medium where they are present. In this paper, we analyze the impact of dust grains on the plasma chemistry of inner cometary comae. As we are mostly interested in qualitative effects of the grain presence in the coma, the simplified model of the cometary coma is used. The comet is located at heliocentric distance equalling 1 AU ($1\,\mathrm{AU} \approx 1.5 \cdot 10^{13}$ cm is the average Earth-Sun distance). Main ionization source for such a coma is photoionization of water molecules by extreme solar UV light ($\lambda < 98.4$ nm). Typical plasma densities considered are $n_e,\ n_i \sim 10^2 \div 10^4\,\mathrm{cm}^{-3}$. This imposes limitations on the neutral densities of interest in our problem; the neutral density is in the range of $n_n \sim 10^{10} \div 10^{13}\,\mathrm{cm}^{-3}$. As density decays with the distance as r^{-2} from the nucleus, the typical size of the region of interest is of the order of 10^3 km.

In this study, we use the gas-to-dust mass ratio equalling unity. A typical size a of dust particles is believed to be $0.3 \div 3\,\mu$m, so the typical dust number density is $n_d \sim 0.1 \div 10^2\,\mathrm{cm}^{-3}$ for the neutral density $n_n \sim 10^{13}\,\mathrm{cm}^{-3}$ of interest here (we assume the mass density of a grain to be $1\,\mathrm{g{\cdot}cm}^{-3}$). As we focussed mainly on the plasma chemical effects of dust grains, we can neglect any transport effects, because dust-induced plasma processes have the shortest timescales. We point out that the cited parameters of the coma are quite realistic (see, e.g., [4 – 7]).

Micro-particles can affect the coma plasma composition via different ways. First, plasma recombination on the surfaces of dust particles can constitute a significant sink of the plasma. This effect, depending on the dust number density, often results in strong depletion of the plasma density. Second, the dust particle surfaces can be the source of electrons due to the photoelectric effect. We note that dependence of the efficiency of the radiation absorption on the refractive index, size of a dust particle, and the radiation wavelength, is quite complex. Figure 1 shows the absorption (scattering) efficiencies $\sigma_{\mathrm{abs/sca}}$ calculated for 121-nm radiation (hydrogen Lyman-α radiation) according to the Mie theory as functions of the dust particle size a. We consider here the Lyman$-\alpha$ line because it is the most important for the photoelectric effect on dust particles, see below eq. (5).

The inset shows the complex refractive index as a function of the photon energy for several compounds (see e.g. [8]). We point to a very small imaginary part of the refractive index k (which determines the absorption of radiation by a particle) in the optical range for ice particles. The values of k for the other compounds under consideration are relatively large. We see that the absorption efficiencies of the radiation are close to 1 for the grain sizes of interest ($a \sim 1\ \mu$m).

Effects of dust particles on the ionization balance in the cometary coma can be estimated from the system

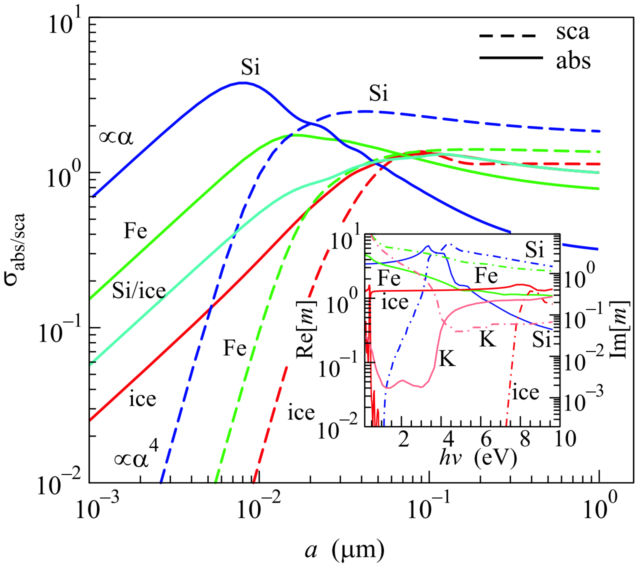

Fig.1. Optical properties of various-composition microparticles as calculated using Mie theory. The efficiencies of scattering $\sigma_{\rm sca}$ and absorption $\sigma_{\rm abs}$ of 121-nm radiation versus the particle size a for various micro- particle materials: ice, iron, silicon, and ice-coated silicon (at the corresponding radius ratio 1:2). The known scaling is shown for small a values ($\sigma_{\rm sca} \propto a^4$ and $\sigma_{\rm abs} \propto a$). The inset shows both the (solid lines) real and (dash-dotted) imaginary parts of the complex refractive index m versus the photon energy $h\nu$ for several compounds that can be present in a dust particle

of the continuity equations for the number densities of electrons n_e and positive ions n_i (H_2O^+, OH^+, H^+, O^+, etc), as well as for the grain charge $Q_d = Z_d e$. In the local approximation, the set of equations is given by [9–11]:

$$\frac{\partial n_e}{\partial t} = q_e - \alpha_m^{\rm rec} n_e n_i^m + \pi\langle \nu_{ed}^{\rm photo} a^2 n_d\rangle - \pi\langle \nu_{ed} a^2 n_d\rangle,$$

$$\frac{\partial n_i^a}{\partial t} = q_e^a - \beta_a n_i^a - \pi\langle \nu_{ad} a^2 n_d\rangle,$$

$$\frac{\partial n_i^m}{\partial t} = q_e^m + \beta_a n_i^a - \alpha_m^{\rm rec} n_e n_i^m - \pi\langle \nu_{md} a^2 n_d\rangle, \qquad (1)$$

$$\frac{\partial Z_d^a}{\partial t} = \nu_d^{\rm photo} + \nu_{ad} + \nu_{md} - \nu_{ed}.$$

Here, we divide positive ions into two distinct groups: the atomic (superscript a) (O^+, H^+, etc) and molecular (superscript m) ions (H_2O^+, OH^+, CO_2^+, etc.). The atomic ions recombine in three-body collisions which can be neglected in comparison with other processes. The recombination coefficient for molecular ions is $\alpha_m^{\rm rec} \sim 10^{-7}\,{\rm cm^3{\cdot}s^{-1}}$. The introduced groups reflect the presence of atomic and molecular positive ions in the inner coma. More detailed plasma chemistry of the cometary coma is not necessary for the current study. The terms ν_{ed} and ν_{jd} ($j = a, m$) describe the losses of electrons as well as atomic and molecular ions on dust particles, respectively; β_a is the conversion rate of atomic ions to molecular ones due to the charge transfer reaction; $q_e = q_e^a + q_e^m$ is the ionization rate due to primary sources of ionization (solar UV radiation, photoelectron, fast particles, etc.) which provide a steady state plasma density in the dustless coma at the level $n_e = n_i \approx \sqrt{q_e/\alpha^{\rm rec}} \simeq 10^2 \div 10^4\,{\rm cm^{-3}}$.

Furthermore, in (1) $\langle ...\rangle$ means averaging over the particle size distribution and $\nu_d^{\rm photo}$ describes creation of photoelectrons when solar radiation is absorbed by a single dust particle with the radius a. Expressions determining ν_{ed} and ν_{jd} can be evaluated by using the Orbit Motion Limited (OML) approach (see e.g. [1, 2]). We have

$$\nu_{ed} = \begin{cases} \pi a^2 \left(\dfrac{8T_e}{\pi m_e}\right)^{1/2} n_e \exp\left(\dfrac{e^2 Z_d}{aT_e}\right), & Z_d < 0, \\ \pi a^2 \left(\dfrac{8T_e}{\pi m_e}\right)^{1/2} n_e \left(1 + \dfrac{e^2 Z_d}{aT_e}\right), & Z_d > 0 \end{cases} \qquad (2)$$

and

$$\nu_{jd} = \begin{cases} \pi a^2 \left(\dfrac{8T_j}{\pi m_j}\right)^{1/2} n_j \left(1 - \dfrac{e^2 Z_d}{aT_j}\right), & Z_d < 0, \\ \pi a^2 \left(\dfrac{8T_j}{\pi m_j}\right)^{1/2} n_j \exp\left(-\dfrac{e^2 Z_d}{aT_j}\right), & Z_d > 0, \end{cases} \qquad (3)$$

where T_e and m_e are the electron temperature and mass, T_j and m_j ($j = a, m$) are the temperature and mass of the j-th ion. In the inner coma, we typically have $T_e \sim T_a \sim T_m \sim 10^2 \div 10^4$ K. Since the charging process strongly depends on the electron-to-ion temperature ratios, T_e and T_j are used as parameters in our model.

The dust induced photoelectric rate $\nu_d^{\rm photo}$ can be evaluated from expression

$$\nu_{ed}^{\rm photo} = \pi a^2 \int\limits_0^{\lambda_W} \sigma_{\rm abs}(\lambda, a, m)\Phi_\lambda Y(\lambda, m, a) d\lambda, \qquad (4)$$

where λ_W is the maximum (threshold) radiation wavelength for the photoelectric effect ($hc/\lambda_W = W$, where W is the work function for a given grain material). For example, λ_W for ice, iron, sodium, potassium, aluminum, and silicon corresponds to the photon energy of

8.7, 4.7, 2.4, 2.3, 4.1, and 4.85 eV, respectively. The photoelectron yield $Y(\lambda, m, a)$ entering into expression for $\nu_{ed}^{\rm photo}$ increases rapidly with the photon energy in the above-threshold region ($|\lambda/\lambda_W| \le 1$) and is often estimated by the expression $Y(\lambda) = Y_\infty(1-\lambda/\lambda^*)$ (see, e.g., [12]), which interpolates experimental data. The characteristic values are $Y_\infty \sim 10^{-2} \div 10^{-1}$ and $\lambda^* \simeq \lambda_W$. It is worth noting that Y increases when the grain size a decreases. For our model, the yield Y appears as an important parameter. We stress that λ_W depends on the charge of the particle, if particle is positively charged only photons with energies $hc/\lambda - W - Z_d e^2/a$ create photoelectrons. In the case of particle with low value of work function W photoelectrons can influence significantly on electron flux onto the particle, because mean energy of photoelectron is usually of the order of a few electronvolts, i.e. much bigger than T_e. For typical comae conditions the photoelectrons thermalize quickly (with the timescale τ_c) in comparison with charging timescales $\tau_{ch} \simeq \pi a^2 n_i v_{Ti} \gg \tau_c \simeq (\nu_{en}\delta_{en})^{-1}$, where ν_{en} and δ_{en} are the electron-neutral collision frequency and the fraction of electron energy lost in a collision. Here we take into account typical values of $\delta_{en} \sim 10^{-1} \div 10^{-2}$ for photoelectrons.

To describe the process of dust charging (and dust induced sinks of both electrons and ions), we employ the OML approach. In this framework, electron and ion currents on an isolated dust grain are determined by using the energy and momentum conservations laws. The currents are calculated by assuming that electrons and ions are collected by the grain if their collisionless orbits intersect the grain's surface. The simple OML analytical expressions for the cross sections of the electron/ion grain interactions are incorporated into above formulas for ν_{ed} and ν_{jd}. In the absence of photoelectric effect, the OML currents lead to the net negative charge on dust because of higher mobility of plasma electrons as compared to that of ions.

The OML approach is fully collisionless, it can be applied when the condition $a \ll \lambda_{Di} \ll \lambda_{Di}^2/a \ll \lambda_{\rm mfp}$ is fulfilled, where λ_{Di} is the ion Debye length and $\lambda_{\rm mfp}$ is the mean-free path of electrons/ions in the neutral gas. The spatial length λ_{Di}^2/a is the characteristic charging length, that is all ion trajectories with the impact parameter $\rho_i \le \lambda_{Di}^2/a$ are closed on the particle's surface. For typical coma parameters λ_{Di}^2/a can (significantly) exceed $\lambda_{\rm mfp}$, so the impact of collisions on the grain charging should be taken into account. It has been shown (see, e.g., [2, 13]) that rare ion collisions increase total ion current on an isolated grain due to ions trapped in the vicinity of the grain, so that the effect results in decrease of the negative dust charge. In collision-dominated regime, the ion current decreases due to strong decrease of the ion mobility, so that the particle negative charge increases (see, e.g. [14]). Within the range of plasma coma parameters (of interest for the current study) both decrease as well as increase of the grain charge are possible. However, the associated change of the charge in comparison with the (collisionless) OML result is not much significant. Moreover, the presence of other dust grains also leads to a change of their charges. Thus, if we take into account decrease of dust charges due to the presence of other grains (interparticle distance $n_d^{1/3} \ll \lambda_{Di}^2/a$), the effects of collisions become less significant and use of the collisionless approach can be justified.

The ionization rate $q_d^{\rm photo}$ induced by the photoelectric effect on dust particles can be roughly estimated from

$$q_d^{\rm photo} \simeq \pi a^2 n_d \sigma_{\rm abs} F({\rm Ly}\alpha) Y({\rm Ly}\alpha, m, a). \quad (5)$$

For the assumed parameters of cometary coma, viz. the dust number density $n_d \simeq 0.1 \div 10^2\,{\rm cm}^{-3}$ and the grain size $a \simeq 1\,\mu{\rm m}$, the value of $q_d^{\rm photo}$ can achieve $10^2 \div 10^4\,{\rm cm}^{-3}{\cdot}{\rm s}^{-1}$, which can be much higher than the steady state ionization rate $q_e \simeq \alpha^{\rm rec} n_e^2 \simeq 0.1{\div}\,{\rm cm}^{-3}{\cdot}{\rm s}^{-1}$ for a dustless coma.

Figure 2 shows results of kinetic simulations for the studied dusty coma. We solve the set of equations (1) numerically for the assumed realistic conditions. The case study presented in Fig.2 shows the dust particle charge Z_d (bottom panel), the electron density n_e (top panel), and the molecular ion density n_m (middle panel) versus the grain number density n_d and the effective (resulting in the photoelectric effect) cumulative solar flux. We can clearly see that strong influence of dust particles on the plasma composition occurs at fairly moderate values of dust number densities $n_d \sim 1\,{\rm cm}^{-3}$. As a result, both depletion and increase of the electron density can be observed in the dusty coma (depending on the grain properties and number density of dust particles) complemented by complicated behavior of the molecular ion component. This ion behavior can be explained by competition of ionization/recombination processes. Indeed, in the case of a positive charge on dust particles, the enhanced (as compared with the steady state level of dustless coma) ion number density can be related to repulsion of ions from dust grains which results in reduced ion losses. On the other hand, increase of electrons leads to increased losses of ions due to recombination processes. Thus the steady state appears as a non-trivial balance of these processes.

The charge on dust particles can be rather large ($|Z_d| \gg 1$), and it can change drastically transport prop-

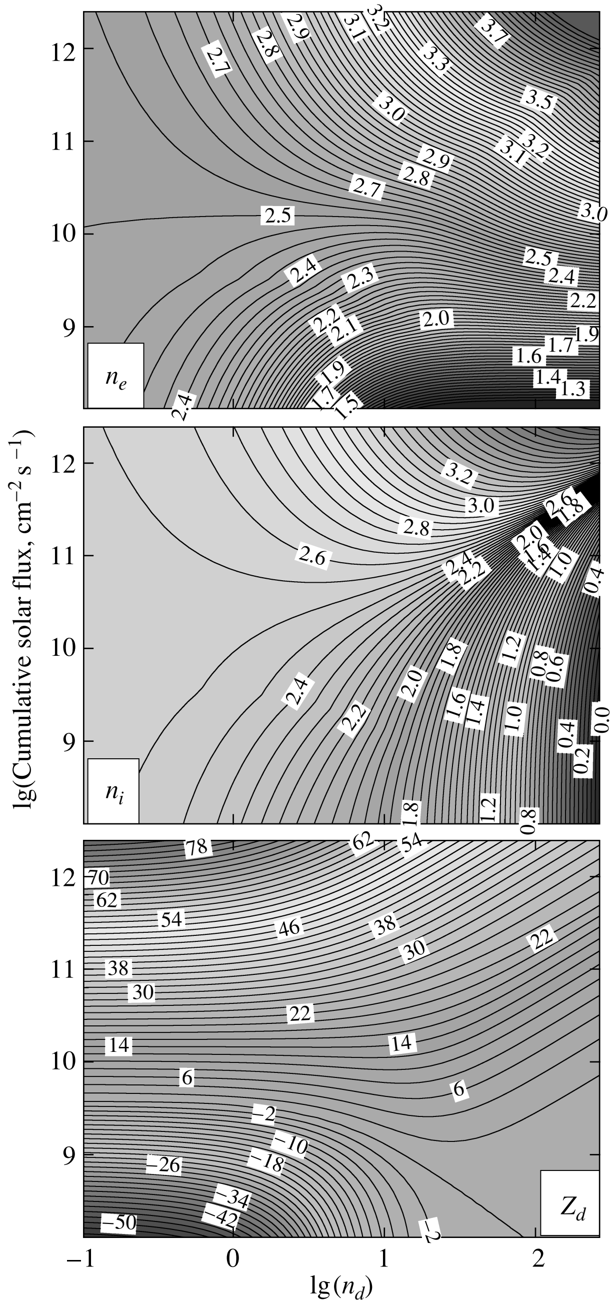

Fig.2. Plasma composition of a cometary coma from numerical simulations of Eq.(1). The dust particle charge Z_d (bottom panel), the electron $\lg(n_e)$ (top panel) and molecular ion $\lg(n_i^m)$ (middle panel) densities of the cometary coma at 1 AU are presented versus the effective solar flux and the dust particle number density n_d. The neutral gas number density is about $10^{12}\,\mathrm{cm}^{-3}$, the dust particle size is 1 μm, the ionization rate is $q_e \simeq 1\,\mathrm{cm}^{-3}\cdot\mathrm{s}^{-1}$. Strong influence of grains on the plasma composition occurs at fairly moderate values of the dust number density n_d

erties of such a plasma. This means that any quantitative analysis of cometary plasma environment (e.g., by using the multiscale MHD model [15]) should take into account the dust-related effects.

We stress that the charge on dust particles can be positive as well as negative, cf. red (upper) and blue (bottom) regions in Fig.2, respectively, depending on the grains photoelectric properties and their concentration. The effect is shown in more details on Fig.3.

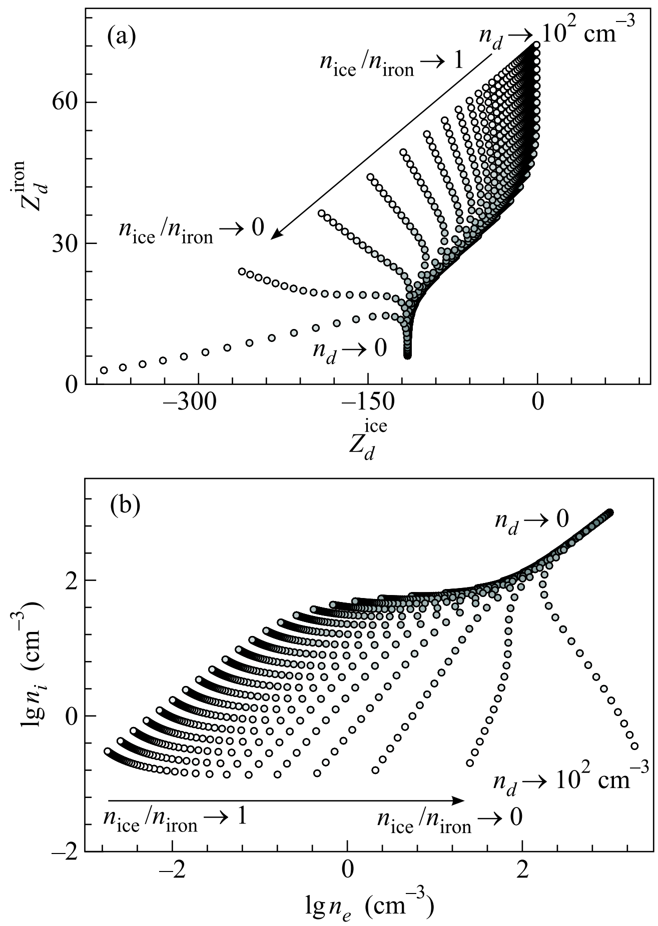

Fig.3. Impact of particle number density n_d and composition (ice/iron) on plasma parameters. Top panel (a) shows the variations of charges of both icy (Z_d^{ice}) and iron (Z_d^{iron}) micrometer size particles versus n_d at different ice/iron particles mixing ratio. Bottom panel (b) shows electron n_e and ion n_i densities at different dust number density n_d and different ice/iron particles mixing ratio

Fig.3 shows case study of the impact of particle number density n_d and composition (ice/iron) on plasma parameters. Top panel (a) shows the variations of charges of both icy (Z_d^{ice}) and iron (Z_d^{iron}) micrometer size particles versus n_d at different ice/iron particles mixing ratio γ_{ii} ($\gamma_{ii} \equiv n_d^{\mathrm{ice}}/n_d^{\mathrm{iron}}$, $n_d^{\mathrm{ice}} + n_d^{\mathrm{iron}} = n_d$). Bottom panel (b) shows electron n_e and ion n_i densities at different dust number density n_d and different ice/iron particles mixing ratio. The value of ice/iron mixing ratio γ_{ii} varies from 0 to 1. It is clearly seen from Fig.3 that both positively and negatively charged particles are present in the coma at wide range of n_d and γ_{ii}.

The effect of bipolar charges on dust particles can result in coagulation of the oppositely charged grains, which in turn makes strong influence on the composition of the coma plasma. Because of relatively strong electric forces, the characteristic times of the coagulation are relatively short. As a result of coagulation, larger particles form, with more probable negative charge residing on them due to plasma absorption (with higher electron mobility). The formed aggregate particles can be of complex fractal shape. It is important that these aggregates are formed directly in coma bulk and not introduced there by expanding neutral gas drag from evaporating nucleus' surface. Recent optical observations [16] support our result on the complex shape of coma grains. In future modeling of cometary environment, the effects of time-dependent distribution of grain sizes (and their influence on the coma plasma) should be taken into account.

To conclude, we have proposed here the kinetic model describing impact of dust grains on cometary comae. We have shown that dust particles, depending on the particle size, number density and photoelectric properties, can strongly affect plasma composition of the dusty cometary coma. It is important that positively as well as negatively charged dust particles can appear in the coma. These opposite charges result in coagulation of dust particles. The shape of these aggregated grains can be complex.

This work was partially supported by the Australian Research Council.

1. S. V. Vladimirov and K. Ostrikov, Phys. Rep. **393**, 175 (2004).
2. V. E. Fortov et al., Phys. Rep. **421**, 1 (2005).
3. S. V. Vladimirov, K. Ostrikov, and A. A. Samarian, *Physics and applications of complex plasmas*, Imperial College Press, London, UK, 2005.
4. M.R. Combi, W.M. Harris, and W.H. Smyth, in *Comets II*, Eds. M. C. Festou et al., Univ. of Arizona, Tuscon, USA, 2004.
5. K. Altwegg, H. Balsiger, and J. Geiss, Space Science Rev. **90**, 3 (1999).
6. S. A. Haider and A. Bhardwaj, Icarus **175**, 196 (2005).
7. S.D. Rodgers et al., in *Comets II*, Eds. M. C. Festou et al., Univ. of Arizona, Tuscon, 2004, p. 505; H. U. Schmidt et al., Comp. Phys. Comm. **49**, 17 (1988).
8. E.D. Palik (ed.), *Handbook of optical constants of solids*, Academic Press, New York, 1998.
9. B. A. Klumov, S. I. Popel, and R. Bingham, JETP Lett. **72**, 364 (2000).
10. B. A. Klumov, G. Morfill, and S. I. Popel, JETP **100**, 152 (2005).
11. B. A. Klumov, S. V. Vladimirov, and G. Morfill, JETP Lett. **82**, 632 (2005).
12. B. T. Draine, Astron. J. Suppl. **36**, 595 (1978); J. C. Weingartner, B. T. Draine, and D. K. Barr, Astrophys. J. **645**, 1188 (2006).
13. S. A. Khrapak et al. Phys. Rev. E **72**, 016406 (2005).
14. S. A. Khrapak, B. A. Klumov, and G. E. Morfill, Phys. Plasmas **14**, 034502 (2007).
15. R. M. Haberli et al., Icarus **130**, 373 (1997).
16. L. Kolokolova et al., in *Comets II*, Eds. M. Festou et al., Univ. of Arizona Press, Tucson, 2004, p. 577.